

# The Effects of LENS Process Parameters on the Behaviour of 17-4 PH Stainless Steel



I. Mathoho, E. T. Akinlabi, N. Arthur, M. Tlotleng and N. W. Makoana

**Abstract** 17-4 PH stainless steel has proven to be one of the workhorse materials in industries such as aerospace, chemical, and energy. The attraction of this alloy to the aforementioned industries is derived from the fact that 17-4 PH stainless steel possesses a combination of excellent mechanical properties and corrosion resistance. Manufacturing of 17-4 PH stainless steel through 3D printing will further inspire confidence in the aforementioned industries. The current study investigated the effects of LENS process parameters on porosity, microstructure, and microhardness. The scanning speed and powder feed rate were varied at 7.62 mm/s-12.7 mm/s and 4.70 g/min-5.98 g/min rpm, respectively, while laser power was kept constant at 300 W. The optimum scanning for both 4.70 g/min and 5.98 g/min was 10.16 mm/s and 12.7 mm/s, respectively. The current study deduced that varying both scanning speed and powder feed rate had an impact on both the microstructure and microhardness.

**Keywords** 17-4 PH stainless steel · LENS · Microhardness · Microstructure · Porosity

## Introduction

Additive manufacturing (AM) also known as 3D printing is a relatively new manufacturing technique, which manufactures parts by building layer upon layer based on the 3D CAD model [1]. Due to the unique dynamics of additive manufacturing, a part produced through AM possesses superior mechanical properties as opposed to a part produced through traditional manufacturing methods [2]. This has attracted industries such as aerospace and biomedical. Laser engineered net shaping (LENS)

---

I. Mathoho (✉) · N. Arthur · M. Tlotleng · N. W. Makoana  
CSIR, Laser Enabled Manufacturing Group, NLC, Pretoria Campus, 0001, Durban, South Africa  
e-mail: [imathoho@csir.co.za](mailto:imathoho@csir.co.za)

E. T. Akinlabi · M. Tlotleng  
Department of Mechanical Engineering Science, Faculty of Engineering and the Built Environment, University of Johannesburg, Johannesburg, South Africa

© The Minerals, Metals & Materials Society 2020  
The Minerals, Metals & Materials Society (ed.), *TMS 2020 149th Annual Meeting & Exhibition Supplemental Proceedings*, The Minerals, Metals & Materials Series, [https://doi.org/10.1007/978-3-030-36296-6\\_45](https://doi.org/10.1007/978-3-030-36296-6_45)

is one of the AM processes, and this process produces parts by depositing powder and irradiating laser concurrently [3]. LENS has the ability to produce functionally graded components and to repair worn out surface, which cannot be achieved by its counterpart processes like selective laser melting (SLM) [3]. However, LENS process has its own fair share of limitations such as poor surface finish and porosity. Therefore, it is imperative to make a proper selection of process parameters, such as laser power, scanning speed, and powder feed rate that will generate a component with minimal defects.

A study by Choi and Chang [4] investigated tool steel characteristics generated by direct metal deposition (DMD). They reported that porosity increased due to increase of powder feed rate; however, they found that porosity decreased as a result of increasing the laser power. This is because of an increase of powder feed rate causes instability in the melt pool, which leads to inducement of porosity. Meanwhile, a study by Lin [5] also investigated the effect of LENS process parameters on porosity of M2 steel. Lin [5] argued that the highest porosity was recorded at the lowest scanning speed employed while the lowest porosity was achieved at moderate scanning speed.

LENS can generate a microstructure, consisting of either columnar grains, equiaxed grains, or a mixture of both. The morphology of the aforementioned grains can be excessively influenced by LENS process parameters [6]. According to Saboori et al. [7] increasing the powder feed rate favours, the formation of equiaxed grains over columnar grains. This is because of partially melted or un-melted powder particles promote heterogeneous nucleation which leads to equiaxed grains [9]. 17-4 PH stainless steel is a precipitation hardened stainless steel which is widely used in industries which includes aerospace, chemical, energy, and biomedical due to its outstanding mechanical properties and corrosion resistance [2].

Since LENS is one of the AM techniques, it is expected that a part generated by LENS possesses higher hardness as opposed to parts generated by traditional methods. This is due to the rapid heating and cooling phenomenon accompanied by Murr et al. [8] reported that the microstructure of 17-4 PH produced on selective laser melting (SLM) is characterized by large martensitic columnar grains along the build direction. On the other hand, Cheruvathur et al. reported [10] that the microstructure of 17-4 PH produced through SLM technique consisted of 50% martensite and 50% retained austenite. However, the proportion of retained austenite was lowered to 10% as a function homogenizing treatment at 1100 °C for two hours followed by air cooling.

The current study aims to investigate the effects of LENS process parameters such as scanning speed and powder feed rate on the metallurgical characteristics of 17-4 PH stainless steel. The metallurgical characteristics include porosity, microstructural evolution, and microhardness. Furthermore, the effect of heat treatment on the microstructure and microhardness will be interrogated.

## Materials and Methods

An argon atomized 17-4 PH stainless steel powder supplied by TLS Technik with particle size ranging from 45 to 90  $\mu\text{m}$  as shown in Fig. 1 was used in the current study.

### *Materials Processing*

The powder was processed on the LENS platform, which uses fibre laser with a maximum power of 1 kw. The scanning speed and powder feed rate were varied while the laser power and percentage overlap were kept constant as shown in Table 1. The aforementioned process parameters were used to print  $20 \times 20 \times 10$  mm coupons. The as-printed coupons were also subjected to homogenizing treatment at 1100  $^{\circ}\text{C}$

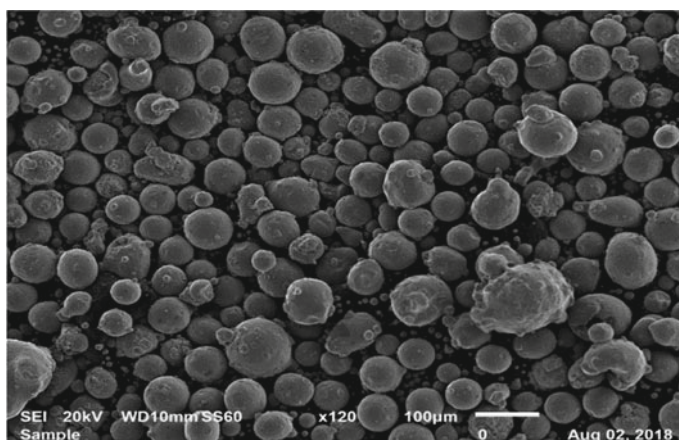


**Fig. 1** 17-4 PH stainless steel powder particles

**Table 1** Process parameters

Sets	Lase power (W)	Scanning speed (mm/s)	Powder feed rate(g/min)	Overlap (%)
1	300	12.7	4.70	50
2	300	10.16	4.70	50
3	300	7.62	4.70	50
4	300	12.7	5.98	50
5	300	10.16	5.98	50
6	300	7.62	5.98	50

for two hours followed by air cooling. Subsequent to homogenizing treatment, the coupons were subjected to aging treatment at 480 °C for one hour followed by air cooling.

## ***Material Characterization***

The image quantitative analysis method was used to measure the porosity of the as-printed coupons. For porosity measurement, the coupons were sectioned, grinded, and polished before being subjected to porosity measurement using the optical microscope. The optical microscope is linked to the image quantitative analysis software. For microstructural evolution analysis, the as-printed and heat treated coupons were sectioned and subjected to metallographic examination procedure which includes grinding, polishing, and etching with FRY'S reagent for 20 s. The optical microscope and the scanning optical microscope were used to analyze the aforementioned samples. Microvickers hardness tester was used to measure the hardness of the as-printed samples and heat treated samples. The load applied is 300 gf for 10 s, and an average of 30 indentations microhardness values was calculated per sample. X-ray diffraction (XRD) technique was used to analyze the phases in an as-printed and heat treated condition. The current and voltage were set at 40 mA and 54 kV, respectively. At a step size of 0.04° within a 2 theta range of 10°–100°.

## **Results and Discussion**

### ***Porosity***

Figure 2 shows the evaluation of the effect of scanning speed and powder feed rate on porosity. It can be seen that for 4.7 and 5.98 g/min powder feed rate, the maximum porosity and minimum porosity were generated at 10.16 and 12.7 mm/s and scanning speed, respectively. The higher porosity at higher scanning speed is probably due to the fact that the melt pool moves fast and does not have enough time to flow and fill some pores. This concurs with a study conducted by Gu et al. [11]. Additionally, it was found that at 5.98 g/min powder feed rate, the porosity decreased with increasing of scanning, wherein minimum of 0.176% was generated at a maximum scanning speed of 12.7 mm/s. The reduction of porosity as a result of increasing scanning speed might be attributed to the fact that at low scanning speeds (7.62 and 10.16 mm/s); there is heat concentration which causes evaporation and induces porosity. Moreover, Fig. 2 shows that 5.98 g/min powder feed rate generated the least porosity than 4.7 g/min for both 10.16 mm/s and 12.7 mm/s except at 7.62 mm/s. Set 2 for 4.7 g/min and set 4 for 5.98 g/min of parameters from Table 1 were found to have generated the lowest porosity.

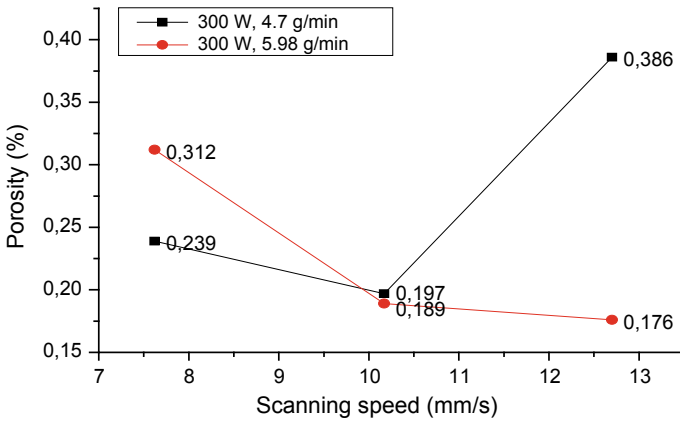


**Fig. 2** A graph of porosity at 4.7 g/min and 5.98 g/min powder feed rate as a function of scanning speed

### Microstructural Analysis

The as-printed microstructure parallel to the build direction is characterized by large alternating columnar grains. These two alternating large columnar grains were found to be different because of one consist of equiaxed grains and while the other consist of small columnar grains. The existence of equiaxed and columnar grains is probably due to 50% overlap, which causes half of re-melting of the previously scanned track [9]. This can be seen clearly in Fig. 3–1. The formation of large columnar grains is due to complex thermal history accompanied by the thermal dynamics of additive

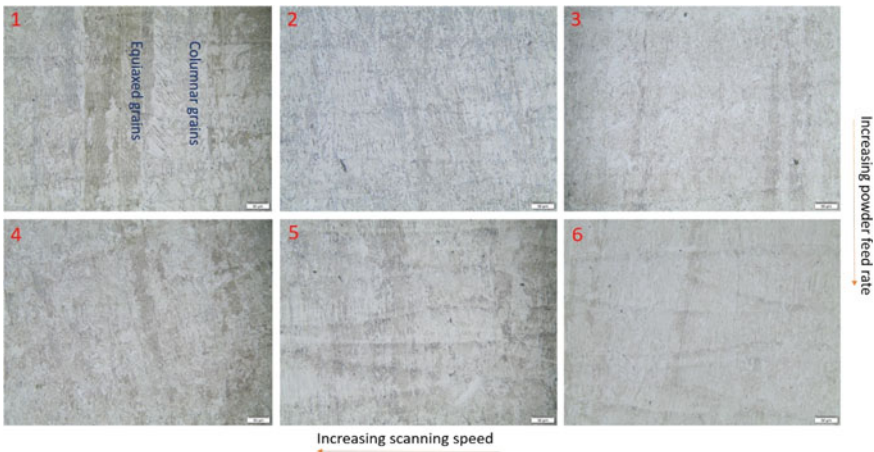


**Fig. 3** As-printed OM microstructures at various sets of process parameters

manufacturing [3]. The microstructure revealed largely martensitic laths with small proportion of retained austenite. Additionally, the presence of overlapping melt pool boundaries can be seen. Figures 1, 2 and 3 represents set 1–3 of process parameters while set 4–6 represent is represented by Figs. 4, 5 and 6. Based on the microstructural evolution evaluation, it was found that the width of larger alternating columnar grain increases as a result of increasing scanning speed. This behaviour is indicative of large thermal gradient that is associated with high scanning speed. Large thermal gradient promotes the formation of large columnar grains due to high cooling rate [12]. Moreover, it was also found that increasing the powder feed rate suppresses the formation of large columnar grains. This attributed to low thermal gradient caused by large amount of powder being deposited, which translates to slow cooling rate [9], which suppresses the formation of columnar grains. The XRD patterns for microstructures in Fig. 3 are shown in Fig. 4, and they show that the amount of retained austenite increases as a function of reducing scanning speed and increasing powder feed rate. This behaviour can be attributed to the fact that the reduction of scanning speed and increment of powder feed rate lead to slow cooling. Since high cooling rate is one of the contributing factors for the formation of martensite, this suggests that slow cooling will favour the retention of austenite.

Only set 2 and set 4 were subjected to homogenizing and aging treatment, and it was established that homogenizing at 1100 °C for 2 h was effective as depicted in Fig. 5. Additionally, XRD patterns in Fig. 6 show that after homogenizing and aging treatment, the microstructure consisted of 100% martensite for both set 2 and set 4. The retention of austenite was suppressed, and this is because of both homogenizing and aging treatment, rapid cooling method (air cooling) was applied. Furthermore, Fig. 5 shows the presence of niobium carbides precipitates (white small phases) after homogenizing and aging treatment. Moreover, after aging treatment the martensitic laths became larger than the martensitic laths in homogenized condition.

### ***Microhardness Analysis***

Figure 7a shows a graph of microhardness as a function of scanning speed for set 1 to set 6 of process parameters. The aforementioned figure indicates that for both 4.7 g/min and 5.98 g/min the microhardness slightly increased with the increment of scanning speed, and this behaviour is ascribed to rapid cooling rate which is promoted by high scanning speed. These results concur with the observed microstructures in Fig. 3, because of increasing scanning speed seems to promote the formation of large columnar grains and suppresses the retention of austenite. Additionally, Fig. 6 exhibits the reduction of hardness of as a result of increasing powder feed rate from 4.7 to 5.98 g/min. The reduction of hardness is because the increment of powder feed rate favours slow cooling rate, which will suppress the formation of large columnar grains as shown in Fig. 3. On the other hand, Fig. 7b displays that for both set 2 and 4, the microhardness after homogenizing treatment decreased. This might be

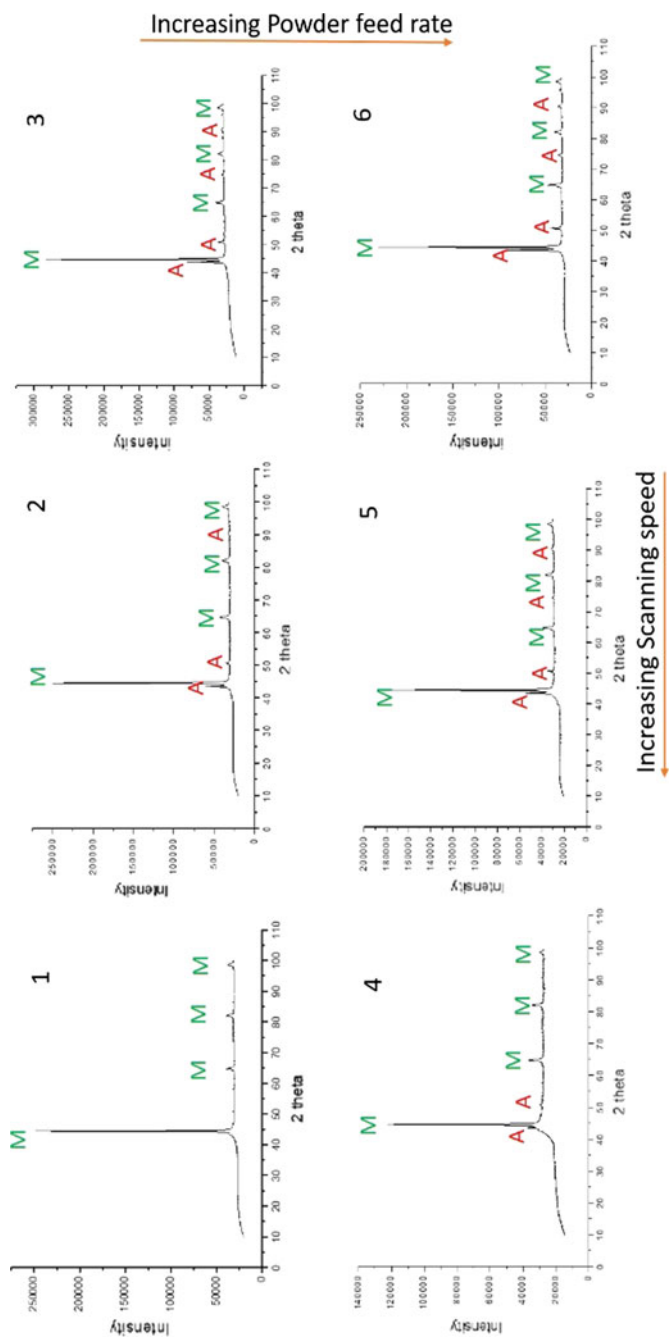


Fig. 4 Various XRD patterns for set 1 to set 6

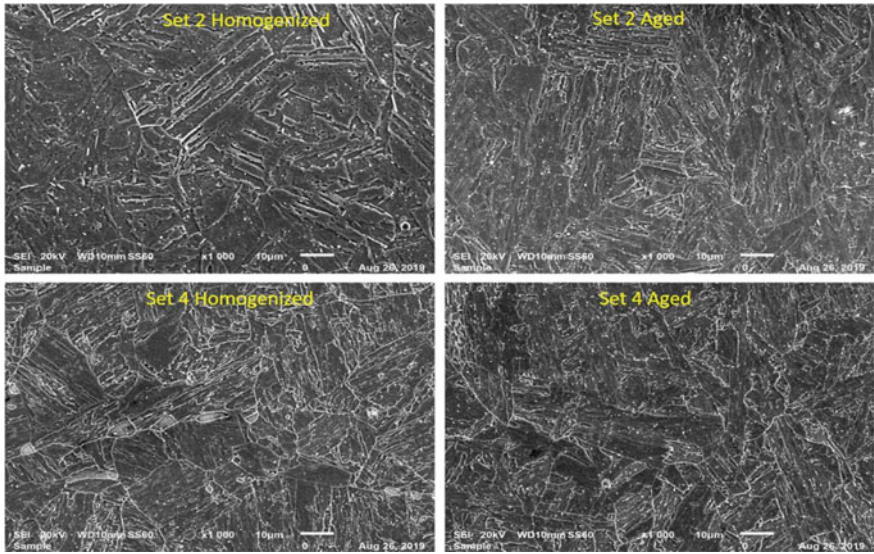


Fig. 5 SEM images of various set 2 and 4 in after homogenization and aging treatment

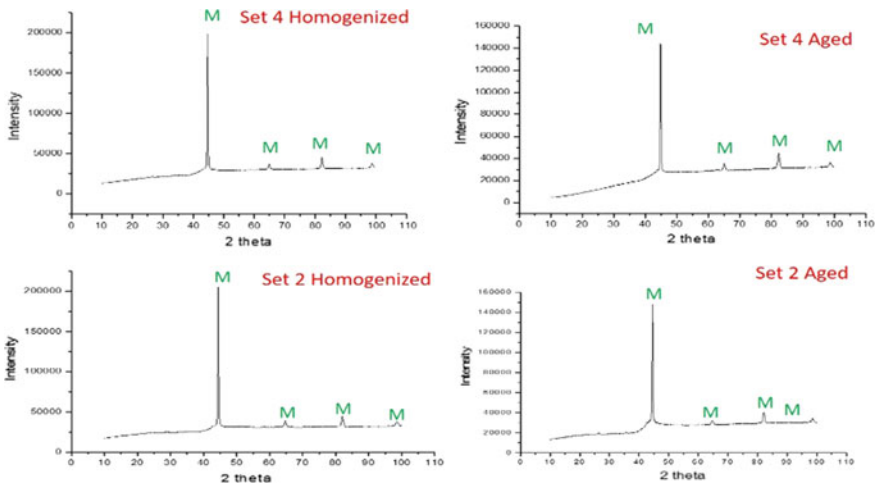


Fig. 6 XRD patterns for set 2 and 4 in homogenized and aged condition

because of copper precipitates, which formed during LENS processing, relocated back into solution. Such copper precipitates are shown in Fig. 8, which shows the SEM image and EDS composition of the copper precipitate taken from set 1 in an as-built condition. The visibility of these copper precipitates invalidates theory; that copper precipitates are small in such a way that they require higher resolution instrument such as transmission electron microscope for identification. However,



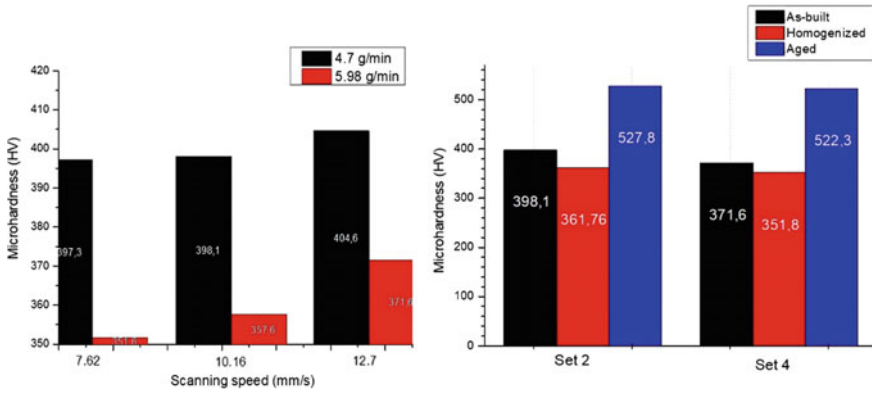


Fig. 7 a Depicting microhardness as a function scanning speed, b depicting microhardness in as-built, homogenized, and aged condition of set 2 and 4

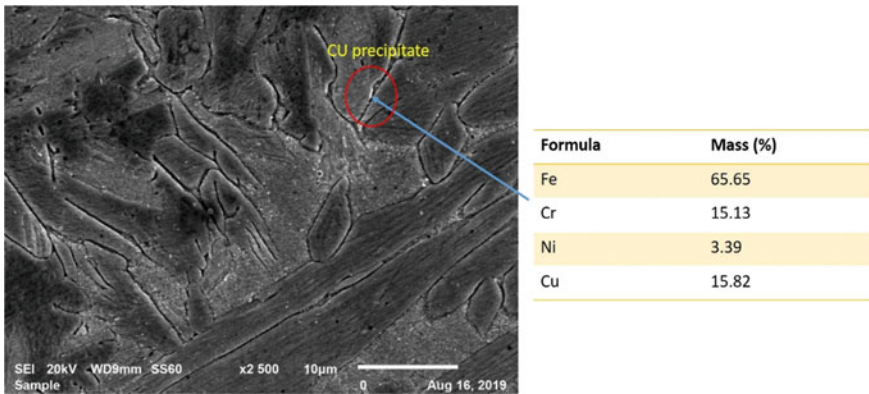


Fig. 8 Depicting SEM images for set 1 in as-built condition

after aging the microhardness increased substantially and this is because of niobium carbides precipitates, which formed during aging as revealed by microstructures in Fig. 5.

### Conclusion

The current study deduced that scanning speed and powder feed rate do have an impact on the porosity during LENS process, wherein increasing the scanning speed had a positive impact on the porosity for 5.98 g/min while for 4.71 g/min increasing scanning speed within a certain range proved to have detrimental effects on porosity. As for the powder feed rate, it was established that increasing powder feed rate at

higher scanning speeds was beneficial in relation to porosity. Additionally, increasing the scanning speed and reducing powder feed rate favoured the suppression retaining austenite. Since additive manufacturing inherently produces a microstructure, which is inhomogeneous, the applied homogenous treatment proved to be effective not only in homogenizing the microstructure but also in suppressing the retention of austenite. Aging treatment also increased the hardness significantly.

**Acknowledgements** Sincere gratitude to the department of Higher Education, Science, and Technology and CPAM for their financial support.

## References

1. Zhu YY, Tang HB, Li Z, Xu C, He B (2019) Solidification behavior and grain morphology of laser additive manufacturing titanium alloys. *J Alloy Compd* 777:712–716
2. Yadollahi A, Shamsaei N, Thompson SM, Elwany A, Bian L, Mahmoudi M (2015) Fatigue behavior of selective laser melted 17-4 PH stainless steel. In: 26th international solid freeform fabrication symposium, Austin, TX, Aug, pp 10–12
3. Saboori A, Gallo D, Biamino S, Fino P, Lombardi M (2017) An overview of additive manufacturing of titanium components by directed energy deposition: microstructure and mechanical properties. *Appl Sci* 7(9):883
4. Song B, Dong S, Deng S, Liao H, Coddet C (2014) Microstructure and tensile properties of iron parts fabricated by selective laser melting. *Opt Laser Technol* 56:451–460
5. Lin J (2017) Effects of the thermal history in additive manufacturing process on the microstructure and hardness of m2 steel
6. Zhu YY, Tang HB, Li Z, Xu C, He B (2019) Solidification behavior and grain morphology of laser additive manufacturing titanium alloys. *J Alloy Compd* 777:712–771
7. Saboori A, Gallo D, Biamino S, Fino P, Lombardi M (2017) An overview of additive manufacturing of titanium components by directed energy deposition: microstructure and mechanical properties. *Appl Sci* 7(9):883
8. Murr L, Martinez E, Hernandez J, Collins S, Amato K, Gaytan S, Shindo P (2012) Microstructures and properties of 17-4 PH stainless steel fabricated by selective laser melting. *J Mater Res Technol* 1(3):167–177
9. Wang T, Zhu YY, Zhang SQ, Tang HB, Wang HM (2015) Grain morphology evolution behavior of titanium alloy components during laser melting deposition additive manufacturing. *J Alloy Compd* 632:505–513
10. Cheruvathur S, Lass E, Campbell C (2016) Additive manufacturing of 17-4 PH stainless steel: post-processing heat treatment to achieve uniform reproducible microstructure. *Miner Metals Mater Soc* 68:930–942
11. Gu H, Gong H, Pal D, Rafi K, Starr T, Stucker B (2013) Influences of energy density on porosity and microstructure of selective laser melted 17-4PH stainless steel. *Solid Freeform Fabrication Symposium* 474:474–489
12. Zhu YY, Tang HB, Li Z, Xu C, He B (2019) Solidification behavior and grain morphology of laser additive manufacturing titanium alloys. *J Alloy Compd* 777:712–716